

Supplementary Information  
High-Resolution, Large Field-of-View, and  
Multi-View Single Objective Light-Sheet  
Microscopy

Bin Yang<sup>1</sup>, Loic A. Royer<sup>1</sup>, and Bin Yang<sup>1</sup>, Alfred  
Millett-Sikking<sup>2</sup>, Merlin Lange<sup>1</sup>, Ahmet Can Solak<sup>1</sup>, Hirofumi  
Kobayashi<sup>1</sup>, Andrew York<sup>2</sup>, Loic A. Royer<sup>12</sup>

<sup>1</sup>Chan Zuckerberg Biohub, San Francisco, USA

September 24, 2020

Chan Zuckerberg Biohub, San Francisco, USA  
Calico Life Sciences LLC, South San Francisco, USA

## 1 Supplementary Note – Optical setup

Supp. Fig. 1a shows a detailed scheme of the optical setup of the microscope. A primary objective (O1, Olympus XLUMPLFLN 20XW NA1.0, water) was used to both generate an oblique light sheet in the sample and to collect the fluorescence. A series of tube lenses (TL1 - TL6) conjugate the pupil pupils of O1 and O2 so that an intermediate image of the sample at the focal space of O1 was formed at the focal space of the secondary O2 (Olympus UPLXAPO20X). The intermediate image has a uniform magnification of 1.33, equaling to the refractive index ratio of that of O1 and O2, so that it is aberration-free [1]. A tertiary objective O3 (Calico AMS 2.0) is oriented by 45° with respect to O2. The fluorescence was filtered by either individual bandpass filters (Chroma ET525/50, ET605/70) or a quad-band filter (Chroma ZET405/488/561/640) and then detected by a scientific complementary metal-oxide semiconductor (sCMOS) camera (Hamamatsu ORCAFlash 4.0). The pixel size of the cameras at the sample space was 219 nm (TL7 - Thorlabs TTL200-A) for PSF calibration and 266 nm (TL7 - Thorlabs TTL165-A) for imaging to be able to capture the desired field of view. O3 was mounted on a piezo stage (PI Fast PIFOC Z-Drive PD72Z1SAQ) so that its focus could be finely tuned.

**Illumination.** The illumination light came out of a fiber output which input is from a custom laser combiner of two lasers (Vortran Stradus 488 nm and 561 nm). The light is firstly collimated by a telescope composed of two achromatic lenses (L1-L2) and then expanded along the horizontal direction by two cylindrical lenses (CL1-CL2). It is further focused on to the 2-axes galvo mirrors by CL3 and then reflected by a dichroic mirror (Chroma ZT405/488/561/640rpc) to be combined with the detection path. The 2-axes galvo mirrors (Cambridge 10 mm 6SD12056) are conjugated with the sample plane so that rotating the two mirrors resulted in a rotation of the excitation beam at the sample plane. In particular, the incident angle of the light sheet at the focal space of O1 can be adjusted by one of the mirrors to 45° with respect to the optical axis. The effective excitation NA is estimated to be about 0.08.

**Optical reflector.** The two switching galvo mirrors shown in Supp. Fig. 1b can create two views at the remote space of the object at the focal space of O1. By adjusting the angles of the two galvo mirrors, the light is reflected either by M5 and M7 or by M6 only. The operating principle is similar to that of a Dove prism. The red arrow is reflected one more time compared to the green arrow. As a result, it is flipped along one direction compared to the green one. The intermediate image of the sample is therefore flipped along the horizontal plane. Supp. Fig. 1c shows two images of a calibration grid taken with the two views, and it clearly shows that the image in the right view is flipped along the horizontal axis compared to the image shown on the left. Moreover, the switching module also changes the incident angle of the light

sheet between  $+45^\circ$  and  $-45^\circ$  since the excitation light also passes through this module. Instead of using galvo mirrors, one can also consider using a mirror mounted on a motorised stage to send the light to different paths. We chose galvos mirrors for these purposes since they are often one order of magnitude or even more faster than motorised stage. It is also possible to have a mirror fold system mounted on a rotating mount. By rotating this module, one would be able to create more than two views of the sample, with in principle unlimited possible views.

**Imaging plane scanning.** A Galvo mirror (Cambridge Tech, 20mm galvo, 6SD12205) was conjugated to the pupil planes of both O1 and O2. Rotating the Galvo mirror scanned the oblique light sheet across the sample (along the x axis), with the incident angle kept at  $45^\circ$ . The Galvo mirror also descanned the intermediate image at the focal space of O2 so that the intermediate image was always projected at the focal plane of O3. Using the galvo for image scan allows faster imaging speed compared to stage scanning. The scanning range is limited to about  $300\text{ }\mu\text{m}$ , both due to cropping of the excitation beam by the relay tube lenses and decreased optical performance when the illuminated plane is away from the optical axis of O1.

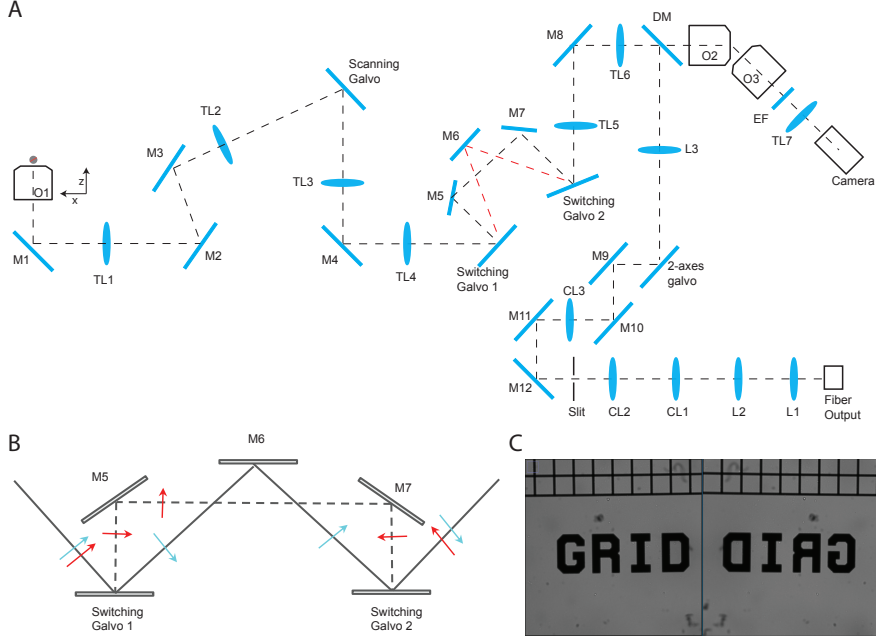


Figure 1: Optical setup of the microscope. **(a)** Detailed layout of the setup. Objectives lenses: O1 - Olympus XLUMPLFLN 20XW, O2 - Olympus UPLXAPO20X, O3 - Calico AMS-AGY v2.0. Tube lenses: TL1, TL2 and TL3 - Olympus SWTLU-C 180 mm, TL4, TL5 and TL6 - 135 mm custom designed tube lens, TL7- Thorlabs TTL200-A or TTL165-A. Scanning galvo and switching galvos: Cambridge 6SD12205 20mm galvo mirrors. Cylindrical lenses: CL1-CL3. Achromatic double lenses: L1-L2. Dichroic mirror: DM - Chroma ZT405/488/561/640rpcv2-UF3. Mirrors: M1-M12, protected-silver coated mirror. 2-axes galvo: Cambridge 6SD12056 10 mm galvo mirrors. EF: emission filters, Chroma ET525/50m or ET605/75m. **(b)** Dual view switching module. The two switching galvo mirrors can switch the light path so that light is reflected either by M5 and M7 or by M6 only. The red arrow is reflected four times along the path and maintains upright, while the green arrow is reflected only three times and becomes inverted. **(c)** Dual view images of a calibration grid (Thorlabs R1L1S1P). The images were taken under bright field illumination and with O3, TL7 and the camera on a straight line with O2.

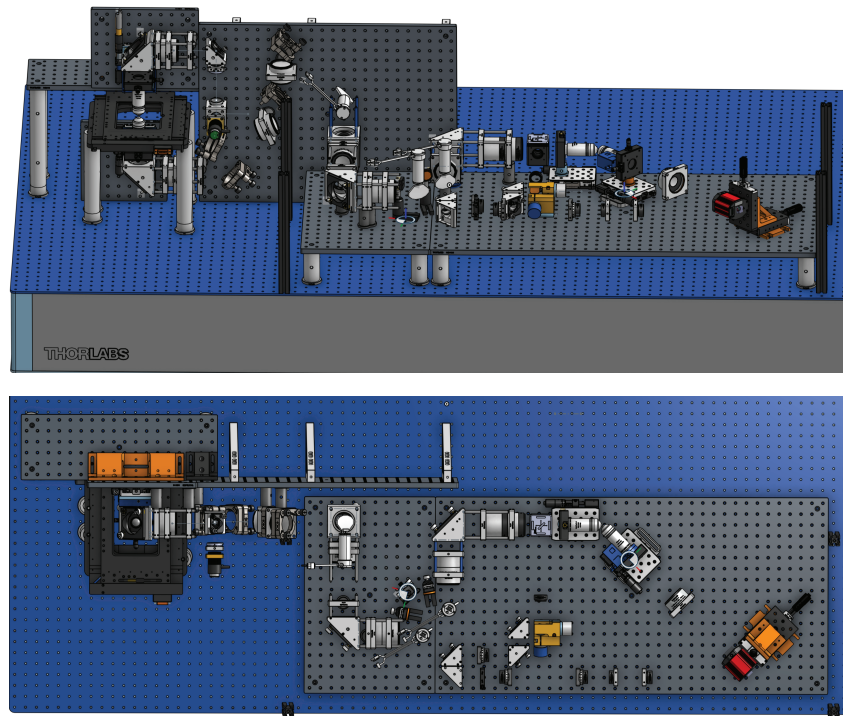


Figure 2: 3D rendering of the optical setup of the microscope. The setup is shown from two different views.

## 2 Supplementary Note – Optical system construction and alignment procedure

### Test samples

1. A multi-frequency grid distortion target (Thorlabs, R1L1S1P) to measure the magnification of the system;
2. A #1.5 glass coverslip (170 um thickness) uniformly coated with the fluorescent dye to characterise the light sheet;
3. 170 nm fluorescent beads embedded in 2% agarose gel to characterise the resolution of the system.

### General remarks and guidelines for alignment

1. There are a few planes are conjugated with 4f-systems in the optical setup. Firstly, the pupil planes of O1, O2, the scanning galvo mirror and the slit are conjugated. The conjugation between the pupil planes of O1 and O2 ensures aberration-free imaging; the conjugation between the scanning galvo mirror and the pupil plane of O1 ensures constant incident angle of the oblique light sheet and proper image descanning; the conjugation between the pupil plane of O1 and the slit allows adjusting the light sheet thickness. Secondly, the 2-axes galvo mirrors and the focal plane of O1 are conjugated so that the incident angles of the light sheet can be adjusted.
2. O1, O2 and O3 are all mounted on translation stages (Thorlabs XR25P) so that their position can be precisely adjusted.
3. Start by placing and aligning all the mirrors at their corresponding locations (either through estimation or follow a CAD design).
4. Then place the lenses one by one, using a reflective mirror at the sample plane to adjust the lateral positions, check the light collimation (with a shear interferometer (Thorlabs SI050) or other means) to adjust the axial positions.
5. Lastly fine tune the system to have diffraction-limited imaging, mostly by assuring proper conjugation between critical planes.

### Detailed alignment procedure

#### Set up all optics

1. Setup the mount for the fibre collimator at desired height.
2. Place mirrors (including the dichroic mirror) after the collimator one by one, ensures that the height is constant and the beam hits the centre of the mirrors. Note that the height is different before and after the two-axes galvo mirrors. Ignore M6 for now, but make sure that the switching galvos are set to the correct value and their value can be adjusted to send light to approximately the centre between M5 and M7.
3. Place a few irises (Thorlabs ID25 and ID50) along the path to aid alignment of lateral positions of the lenses.
4. Make sure that the light passes through the mount of O1 centered.

5. Place a reflective mirror at the place of O1, slightly adjust M1 so that the reflected beam passes all the iris centred. Go back to step 4 if necessary.
  6. Place L1 and L2 to have a collimated beam.
  7. Place TL1, adjust its lateral position so that the reflected beam passes all the iris and its axial location is approximately at the desired location.
  8. Place TL2, adjust its lateral position so that the reflected beam passes all the iris, adjust its axial position so that the beam is collimated after TL1.
  9. Repeat step 8 for TL3 to TL6.
  10. Start with having O2 and O3 along a straight line. Make sure the reflected light passes through the centre of the mounts of O2 and O3, then place O2 and O3 in the setup.
  11. Place TL7 in the setup, make sure that the light passes through its centre.
  12. Place the camera in the setup, depending on the specificity of TL7, make sure the distance from TL7 to the camera sensor is correct.
  13. Place O1 in the setup.  
**Adjust the position of O1 and O2 to have them both conjugated to the galvo mirror.**
  14. Send a sinus wave signal to the scanning galvo, adjust axially O1 so that the light coming out of it is scanning laterally without changing angles. This is the desired position for O1.
  15. Put the grid sample on the sample stage. If necessary, add a spacer beneath it so that O1 is approximately at its desired position.
  16. Use a flash light to illuminate the grid and have its image on the camera.
  17. Move O3 200 µm away and closer to O2, and measure the magnification of the system with the grid. The goal is to have the same magnification regardless of the relative position of O3 to O2. Move O2 and O3 together axially until at one point the magnification is uniform. The pupil plane of O2 is then conjugate to that of O1.
  18. Translate the stages to move O2 and O3 together axially until at one point the magnification is uniform.
  19. Place a sample with beads imbedded in 0.5% agarose on the sample stage. Place the emission filter, switch on the laser and observe the fluorescence image of the beads. The defocused image of the beads should look circular, otherwise slightly adjust O2 laterally to have a circular image of the beads. Adjust O3 slight to bring back the field of view to the centre of the camera. One can move O3 axially to inspect the images of the beads along different z. The image quality should be constant across at least 500 µm, otherwise the alignment is subject to further trouble shooting and improvement.
- Dual view component alignment.**
20. Adjust the voltages sent to the switching mirrors so that the light is reflect to the centre of the M6 and also passes through the irises from M6 to O1 thought the centre.
  21. Place the grid back to the sample stage and measure the magnification with O3 at 200 µm away and closer to O2. Translate the stage to move M6 so that the magnification is uniform when translating O3 axially.
  22. Repeat step 20.

### **Oblique light sheet setup and alignment.**

23. Place O3 and the components downstream at  $45^\circ$  to O2. Place a sample with beads imbedded in 0.5% agarose on the sample stage. Adjust O3 so that the fluorescence image of the beads is capture by the camera in the centre of the field of view.
24. Set up CL1 and CL2 so that the laser light is expanded along the direction horizontal to the optical table.
25. Set up CL3 so that the beam is focused on the 2-axes galvo.
26. Place the slit at approximately the focal plane of CL3.
27. Place L3 so that the light becomes collimated again along the vertical direction.
28. Place a sample with beads imbedded in 0.5% agarose on the sample stage. Adjust the sample of the y-axes galvo to adjust the incident angle of the light sheet to  $45^\circ$  within the xy plane. Adjust O3 slightly to refocus if necessary. When the light sheet is at the correct angle, all beads in the image will appear in focus.

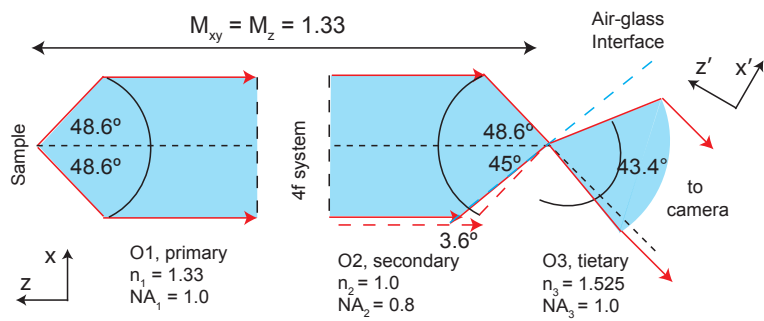


Figure 3: Diagram illustrating the effective detection NA along the  $x'$  axis. Blue shades indicate the light cone collected by each objective; black arcs indicate the extent of the NA (full-aperture angle  $2$  of each objective); red lines represent the light rays with the highest incident angle; black dashed lines show the optical axis. The intermediate image at the focal space of  $O_2$  is magnified by 1.33 (equal to  $NA_1/NA_2$ ) along both the lateral and axial directions to minimize the aberration of the intermediate image. The blue dashed line indicates the position of the air–glass interface. All the light passing through  $O_2$  is refracted at this interface and enters  $O_3$ , with the exception of only a small portion of the light being cropped by the interface (left side between the blue and red dashed lines). The effective detection NA along the  $x'$ -axis is  $1.33 \times 1.525 \times \sin(43.4^\circ/2) \approx 0.75$ . The effective NA along the  $y$  axis is 1.0, since light is not cropped along this direction.

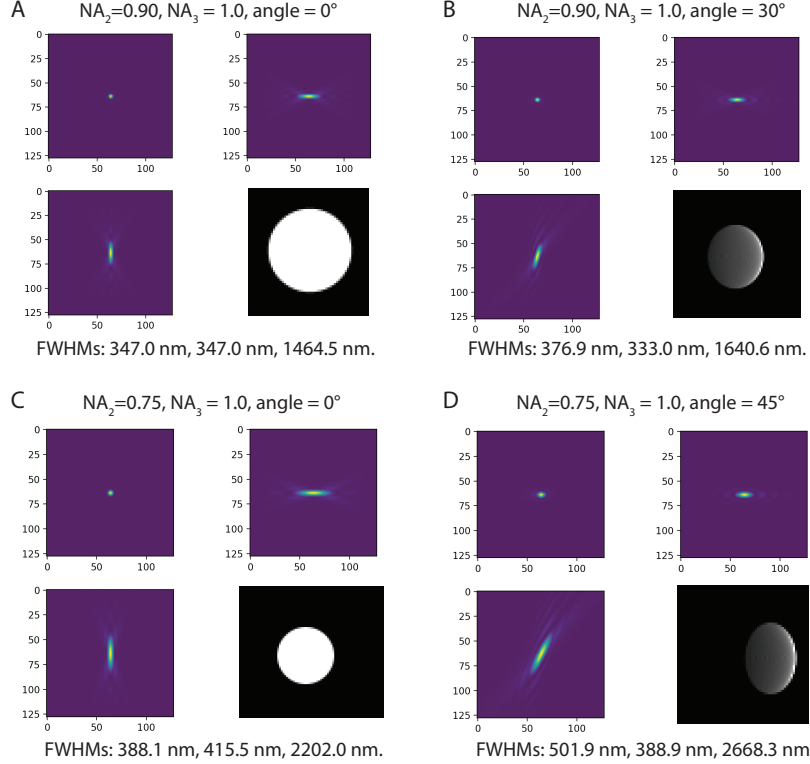


Figure 4: Simulated PSF and pupil function of the eSPIM system. The eSPIM system is simplified to only consider O2 and O3. A plane wave enters O2 and the pupil function is estimated after it exits O3. The 3D PSF is then simulated from the pupil function. O2 (NA 0.75 or 0.9) and O3 (NA 1.0) are respectively air and solid immersion objectives. They are either along a straight line (i.e. angle = 0°) or orientated by an angle (30° or 45°) between their optical axes. (a) and (b) show the simulated PSF (xy, xz and yz cross sections are shown) and pupil function (gray images) for a high NA version of eSPIM, similar to reported in [2]. (c) and (d) show the simulated PSF and pupil function for a system similar to that presented in this paper. When the angle between the two objectives is not 0°, the effective pupil function of this imaging system show a compression of the light towards one direction. The resulting PSF is therefore not straight along the z axis, but has an angle to it, which is 17° for (b) and 27° for (d). The FWHMs of the PSFs are given at the bottom of the images, for the three principle axes. The FWHMs along y are comparable with O2 and O3 either along a straight line or tilted. The FWHMs along the two other directions are slightly wider when the two objectives are tilted.

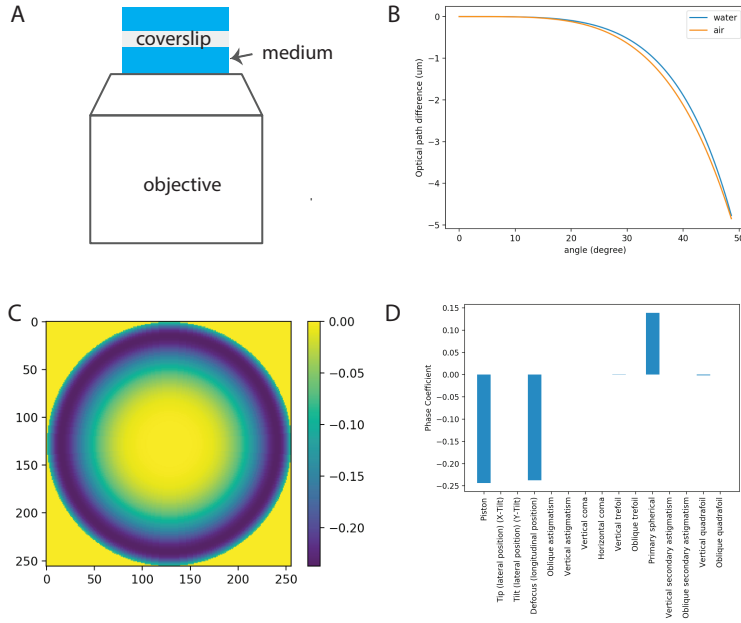


Figure 5: Optical path difference when placing a coverslip into a medium. **(a)** shows an optical system where a coverslip is inserted into the imaging medium of an objective. Depending on the type of the objective, the medium could be air, water, immersion oil, and etc. **(b)** plots the optical path length of an emitter at the coverslip surface as a function of the angle between the emission ray and the optical axis, in the case of air or water medium. **(c)** shows that 2D map of the optical path difference of using air and water medium. This 2D phase map is then fitted with the first 50 Zernike terms. **(d)** shows the coefficients of the first 20 Zernike terms. The major non-zero Zernike terms are piston, defocus and primary spherical aberration. Note: The Zernike fitting is done using pyOTF, a simulation software package for modelling optical transfer functions (OTF)/point spread functions (PSF) of optical microscopes written in python. Link: <https://github.com/david-hoffman/pyOTF>

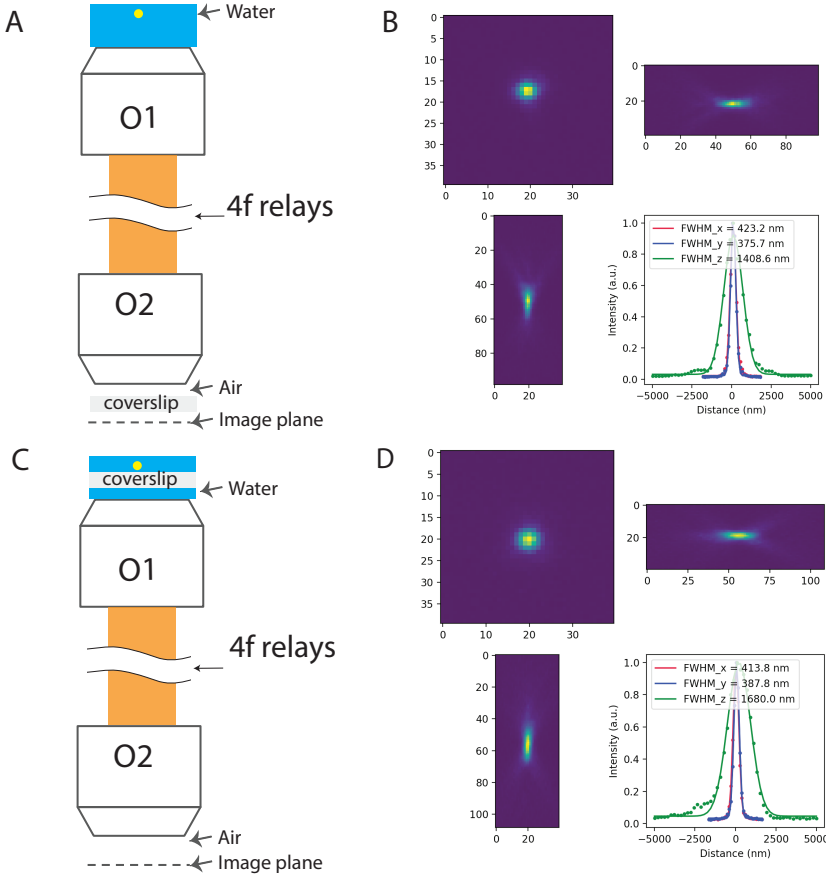


Figure 6: Converting a water dipping objective into a water immersion objective using remote focusing. (a) shows a remote focusing system composed of two objectives whose pupil planes are conjugated by a 4f relay system. Yellow dot: fluorescent bead. O1: 20x, 1.0NA, water dipping. O2: 20x, 0.8NA, air. O1 should be used directly facing the sample without any coverslip in between. O2 requires a coverslip between the objective front lens and the image plane. (b) shows the PSF of the system shown in (a) measured with 170 nm yellow fluorescence beads. Interestingly, according to Supp. Fig. 5, one can instead place the coverslip at the focal space of O2 to that of O1 as shown in (c), the only aberration term introduced is slight primary spherical aberration which can be compensated by translating one of the relay lenses in the 4f system. (d) shows the PSF of the system shown in (c) measured with 170 nm yellow fluorescence beads, which is practically the same as shown in (b).

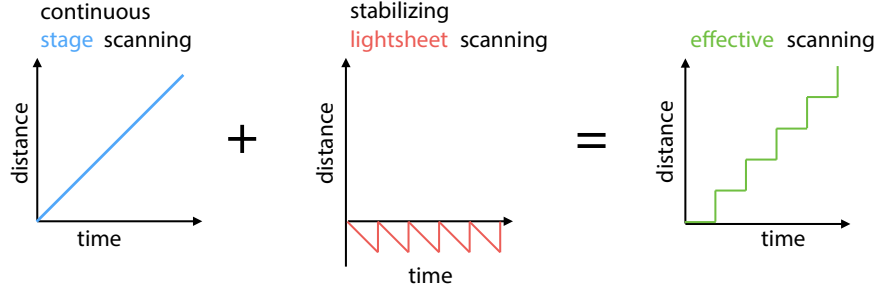


Figure 7: Light sheet stabilized stage scanning. During the acquisition of a 3D image stack, the stage moves continuously and the galvometer scanner performs a counteracting motion of the light-sheet and detection planes to cancel out any relative motion between sample and imaging plane, resulting in an effective step-wise scan of the sample.

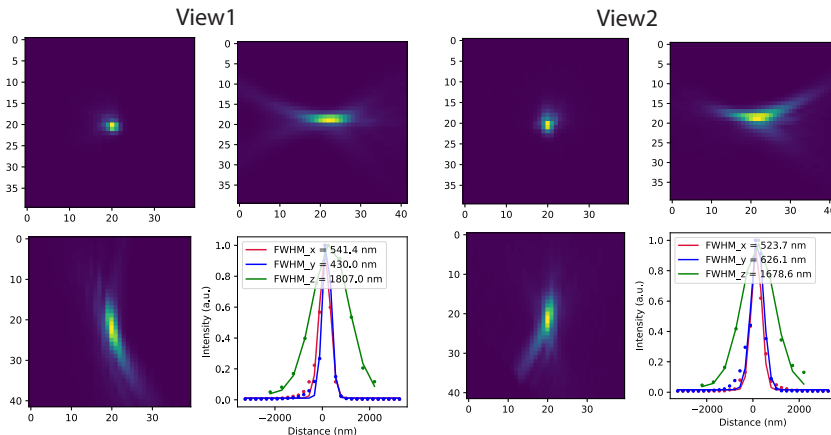


Figure 8: Point spread function of the microscope measured using 170 nm green fluorescence beads. Fluorescence beads are embedded in 0.5 % agarose gel. Top rows: xy and yz cross sections. Bottom rows: xz cross section and fitted xyz profiles.

### 3 Supplementary Note – AMS-AGY v2.0 Objective – Full technical details and context

[TODO: add references]

Light-sheet fluorescence microscopy (LSFM) or selective plane illumination microscopy (SPIM) is a powerful technique for biological imaging. Fast, gentle, and with good sectioning, the idea has seen much attention with innovations like the DiSPIM and Lattice, and commercial instruments like the Zeiss Lightsheet 7 and the Leica DLS. However, traditional light-sheet designs require two or more orthogonal lenses for illumination and collection, resulting in an awkward interface between the biology and the optics, and a major drawback for many users and applications.

The Oblique Plane Microscope (OPM) invention of 2008 restored the traditional coverslip boundary by passing light-sheet excitation and emission through a single primary objective, and then using a tilted remote refocus (RR) in the downstream optics to image the equally tilted plane of illumination (the object plane). OPM showed that light-sheet microscopy could be done with a standard microscope and sample interface, but seemingly exchanged this convenience for heavy losses in resolution and optical efficiency.

The problem with OPM was that the tilted portion of the remote refocus would lose a significant fraction of the emission light, simply because the numerical aperture of the final objective was too low. An ideal objective for this location would collect all of the emission light, even with the additional tilt imposed by the OPM architecture, i.e. a full hemisphere of collection (a seemingly impossible requirement when objective half angles are typically limited to 70 deg).

However, in 2018 the Epi-illumination SPIM microscope (eSPIM) showed that the major optical losses in OPM-style systems could in fact be avoided. By using a water objective and coverslip assembly as the final objective, the numerical aperture could now equal the refractive index of air (1.0) i.e. the ‘immersion medium’ of the opposing objective in the remote refocus. This is the crucial insight: to make the elusive ‘hemisphere’ collection objective you simply need a numerical aperture that is greater than (or equal to) the index of the medium in which it operates. So for example, an NA 1.0 water immersion objective has a modest 49 deg collection cone in water (a reasonable lens to manufacture), but in air this transforms to 90 deg. So by imaging at the coverslip boundary, a water lens can indeed collect a solid angle of 2pi from an air medium.

There are however some additional considerations that complicate the eSPIM approach. The tertiary objective assembly is corrected for a water/coverslip/water medium (not water/coverslip/air). It can perform well if operated exactly at the surface of the coverslip, but deviations in alignment that push the image into the coverslip (or out into the air) will produce strong aberrations, so it can be challenging to align and keep stable (and hydrated). In addition, the bulkiness of the coverslip-water assembly requires longer working distance objectives in the remote refocus to avoid mechanical collision from the tilt. In practice this

limits the choice of optics (and tilt range) and can force a reduced numerical aperture on the air objective.

Inspired by OPM and eSPIM, the AMS-AGY v1.0 objective (aka Snouty) was developed to eliminate the previous trade-offs and compress the opto-mechanical difficulty into a single dedicated component (Fig. 9B). The NA 1.0 objective features a monolithic glass tip with zero working distance; this tip is optically equivalent to an oil/coverslip/air interface but alignment-free and mechanically stable. The tip also features an anti-reflection coating to maximize collection from the full hemisphere of rays (as noted previously NA 1.0 in an air collects from the full 90 deg half-angle). The zero working distance is another critical feature; the large refractive index mismatch at the glass-air interface produces strong spherical aberrations that vanish only at this boundary. The high refractive index of the glass tip compresses the collection half-angle so the tip can be shaved off (Fig. 10B) to allow a range of tilt angles from 0-45deg. This excellent mechanical clearance allows image collection as close as 100um from a planar boundary. In practice this means the AMS-AGY objective can be paired with objectives with the highest numerical apertures and therefore the maximum collection efficiency. Infinity and color corrected, this component enables an extensive suite of design options as detailed in the High NA single-objective light-sheet (SOLS) article of 2019.

The Snouty v1.0 objective enabled ‘bolt-on’ SOLS designs with uncompromised numerical aperture, and is the ideal microscope for many light-sheet applications. However, the design of the v1.0 lens was constrained by mechanical and economic considerations, ultimately limiting the field of view (FOV) to 150um diffraction-limited (250um to the shaved edge, Fig.10B). The economic argument is obvious: manufacturing difficulty and cost typically increase with field of view, and a costly lens would increase the prototyping risk and lower uptake of the technology. The mechanical limitations are more subtle; for the highest numerical aperture SOLS designs, the air objective that opposes the Snouty lens in the remote refocus can have working distances as short as 200um (Fig. 10B). So as the Snouty lens is tilted, the field of view (housed in glass) moves towards a collision with the opposing lens i.e. the Snouty FOV competes directly with the working distance of the paired objective in the remote refocus.

To overcome the limits on field of view the Snouty v2.0 prototype (aka KingSnout) was developed with a 3x boost on FOV compared to the v1.0 lens i.e. 450um diffraction limited and 450um to the shaved edge (Fig 1A, 2A). The large field was partly achieved by increasing the budget for design and manufacture (it is a larger and more complex lens) but also by eliminating the margin between the diffraction limited FOV and the shaved edge. This enables the lens to be used ‘off-axis’ in the tightest of spaces without losing optical quality. Snouty v2.0 is also ground at a more aggressive angle (55 deg vs 45 deg) which combined with the reduced margins gives the maximum clearance for tilting in the remote refocus. It is a strict upgrade to the v1.0 objective and compatible with all SOLS designs.

The discussion of lens specifications brings to the forefront some important considerations that should be emphasised. The AMS-AGY objectives are ex-

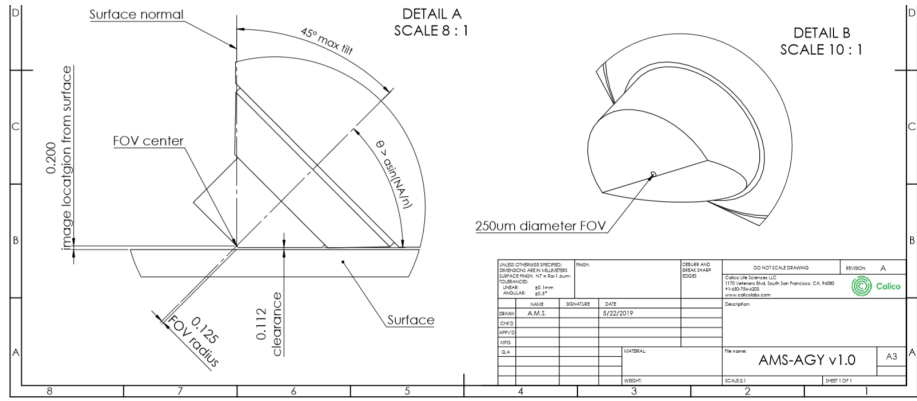


Figure 9: Technical drawing for AMS-AGY V1.0 objective.

actly as specified: NA 1.0 with fields of 150um (v1.0) and 450um (v2.0), where NA 1.0 actually means the lens will image stigmatically at NA 1.0, not that it merely collects at this NA. How these specifications translate into the object space and the resulting volumetric imaging performance is subtle and beyond the scope of this section. However it should be noted that these objectives can be used beyond the specified fields, by up to a factor of approximately 1.7x, but not at NA 1.0. So a less genuine, but perhaps more typical specification would be NA 1.0 with fields of 250um (v1.0) and 750um (v2.0) and is something to bear in mind when considering a SOLS design.

Availability and dissemination is crucial for the impact of any technology. The Snouty v1.0 lens is commercially available thanks to investments of time and money from Applied Scientific Instrumentation (ASI). It may not yet be obvious to ASI if a similar investment in Snouty v2.0 is justified. Their decision will depend on your input; if you would like one of these lenses, please contact Jon Daniels at ASI.

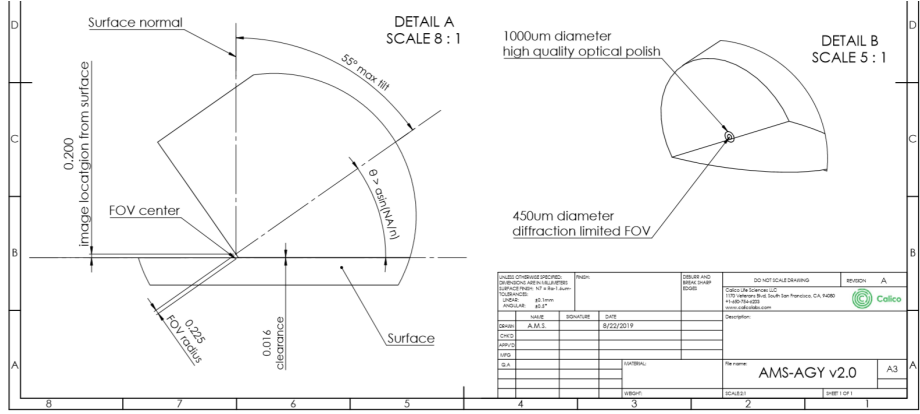


Figure 10: Technical drawing for AMS-AGY V2.0 objective.

## References

- [1] Botcherby, E. J., Juskaitis, R., Booth, M. J. & Wilson, T. Aberration-free optical refocusing in high numerical aperture microscopy. *Optics Letters* **32**, 2007–2009 (2007). URL <http://www.osapublishing.org/abstract.cfm?uri=ol-32-14-2007>.
- [2] Yang, B. *et al.* Epi-illumination SPIM for volumetric imaging with high spatial-temporal resolution. *Nature Methods* **16**, 501 (2019). URL <https://www.nature.com/articles/s41592-019-0401-3>.